Sulfate attack of deep foundation concrete: New testing method and influence of temperature on degradation mechanism

Faten Souayfan, Farah Kaddah, Sonia Boudache, Stéphane Guerineau, Christophe Justino, Emmanuel Roziere

Case Studies in Construction Materials 23 (2025) e05368

Contents lists available at ScienceDirect

Case Studies in Construction Materials

journal homepage: www.elsevier.com/locate/cscm

Sulfate attack of deep foundation concrete: New testing method and influence of temperature on degradation mechanism

Faten Souayfan [a,b], Farah Kaddah [a,c], Sonia Boudache [a], Stéphane Guerineau [b], Christophe Justino [b], Emmanuel Roziere [a,*]

[a] Civil engineering and Mechanics Research Institute, Nantes Université, École Centrale de Nantes, CNRS, GeM, UMR 6183, Nantes 44000, France
[b] Soletanche-Bachy, Chemin des Processions, Montereau Fault Yonne 77130, France
[c] Research and Innovation Center on CO2 and H2, Khalifa University of Science and Technology, Abu Dhabi, United Arab Emirates

ARTICLE INFO

Keywords:
Thaumasite sulfate attack
Supplementary cementitious materials
C_3A content
Limestone filler

ABSTRACT

Thaumasite attack presents a significant concern within the domain of deep soil foundation construction. In these exposure conditions, concrete is exposed to sulfate-rich groundwater from the fresh state, hence the need for specific durability testing procedure. The use of supplementary cementitious materials (SCM) has long been a way to prevent external sulfate attack. The specific degradation due to thaumasite sulfate attack (TSA) at 5 °C mitigates the observations made for the use of SCM at 20 °C. In response to these challenges, a new testing method has been developed and 41 cement-based binder mixtures, encompassing diverse supplementary cementitious materials (SCM), fillers, and variable C_3A contents, were tested at 5 °C and 23 °C. Their behavior at 5 °C was consistent with the phenomenology of TSA: visual deterioration, and significant mass loss of several specimens up to −9 %. The presence of thaumasite at 5°C was substantiated through SEM and XRD analyses. The measurements at 5 °C indicate that length variations are not a fully reliable parameter to assess the resistance to TSA: a sample with low length variation (0.1 %) had a mass variation of 6 %, indicating a significant degradation. The joint use of mass and length variations as indicators thus offers valuable insights into the identification of optimal composition for cement-based materials regarding their resistance in deep foundation exposure conditions.

1. Introduction

Thaumasite attack presents a significant concern in the context of deep foundation construction [1]. The structural elements are often exposed to harsh environmental conditions, including high moisture content and varying temperatures during concreting. The presence of sulfate ions in groundwater is likely to increase the risk of thaumasite formation, which can lead to cracking, spalling, and the formation of non-cohesive mass in concrete [2,3]. Thaumasite ($Ca_3Si(OH)_6(CO_3)(SO_4)\cdot 12\ H_2O$) has been reported to develop primarily under specific conditions, notably at a temperature lower than 15°C, an abundant presence of calcium silicate, sulfate, and carbonate ions, along with a high level of moisture [4,5]. The process of thaumasite formation can occur through two main pathways: direct and indirect [2]. In the direct pathway, thaumasite is created through the reaction of calcium silicate hydrate (C–S–H) with calcite in the presence of moisture and free sulfate ions. Alternatively, the indirect route involves the precursor role of ettringite in the formation of thaumasite. When water containing sulfate ions is present, ettringite is initially formed and subsequently reacts with

* Corresponding author.
E-mail address: emmanuel.roziere@ec-nantes.fr (E. Roziere).

https://doi.org/10.1016/j.cscm.2025.e05368
Received 3 July 2025; Received in revised form 12 September 2025; Accepted 30 September 2025
Available online 1 October 2025

C–S–H and carbonates/bicarbonates to produce thaumasite. As thaumasite forms at the expense of the C-S-H gel, the hardened cement paste progressively loses its binding ability [6,7].

The inclusion of carbonates during the process of thaumasite formation raises concerns about the potential deterioration of Portland-limestone cements, as defined in the European standard EN 197–1:2011 [8]. Previous research has demonstrated that concrete made using ordinary different Portland-limestone cements is susceptible to damage when exposed to sulfate solution at low temperatures [7,9] According to the American and Canadian standards [10,11] Portland-limestone cement can include up to 15 % of limestone. EN206 European standard [12] limits the use of Portland-limestone cements with limestone content ranging from 6 % to 20 % by cement mass in moderate sulfate environments. In the UK, the Thaumasite Expert Group (TEG) reported that cements containing limestone filler ranging from 6 % to 35 % should not be allowed in conditions where sulfate concentrations in groundwater exceed 0.4 g/L [13]. CSA A23.1 (2009) [14] has prohibited the use of Portland-limestone cement in sulfate-rich environments.

The use of Supplementary Cementitious Materials (SCM) is a prevalent method to reduce the risk of thaumasite Sulfate Attack (TSA) [15]. Pozzolanic admixtures react with the calcium hydroxide in the hydrated cement paste, resulting in the formation of secondary hydration products and a decrease in the calcium-to-silicon ratio within the C-(A-)S-H phase. Hydrated cement phases with reduced calcium hydroxide content demonstrated better resistance to Thaumasite Sulfate Attack (TSA) [16]. Based on this observation, the Canadian standard CSA A3001–10 recommended incorporating minimum specified proportions of SCM into Portland-limestone cement to ensure adequate sulfate resistance. However, it was demonstrated that these minimum proportions of slag, metakaolin, and fly ash were insufficient to produce a highly sulfate-resistant blended Portland-limestone cement (PLC) [15]. Increasing the content of SCMs in PLC blends beyond the standard recommendations for slag and metakaolin resulted in achieving the required resistance level. Additionally, it was found that none of the blends containing Type F fly ash showed expansion levels below the standard limits [16]. On the other hand, the data collected from PCA of American cement manufacturers revealed that the current CSA standard, specifically the CSA A3004-C8 Procedure B conducted at 5°C, with a sulfate concentration of 50,000 mg/L, was too severe comparing to actual in situ conditions [17].

They showed that mortars with and without limestone experienced expansion and failure, with the formation of gypsum and ettringite for samples stored at 5 °C. This finding is significant as it demonstrates that thaumasite sulfate attack, distinct from minor thaumasite formation in air voids, did not initiate the deterioration; rather, it occurred in non-sulfate-resistant systems only after ettringite had caused the primary degradation.

The ASTM C1012 [18] standard is commonly used to evaluate the durability of cement-based materials exposed to external sulfate attack. Previous research has pointed out the limitations of this standardized TSA test in effectively assessing the risk of TSA at 5 °C. This has led to an aggressive approach compared to the actual behavior of concrete, resulting in the formation of ettringite and gypsum instead of thaumasite, which caused significant failure and deterioration [17]. As a result, the primary objective of this study was to develop an experimental protocol capable of evaluating the TSA risk specifically for concrete in constant and direct contact with sulfate-rich groundwater. Its primary purpose is to address and mitigate the risks associated with using limestone filler as a mineral addition in deep foundation concrete. The concrete specimens were subjected to both external and internal sulfate exposure, simulating potential sources of sulfate that may be present in the real-world application of deep foundation concretes. The conditions of this proposed protocol were carefully chosen to replicate closely the actual exposure conditions of concreting in deep foundations. Previous studies have highlighted the difficulty in differentiating between the effects of thaumasite precipitation and ettringite precipitation. In this regard, the protocol developed does not rely solely on length variation over time as an indicator, but also on mass variation.

This new innovative test was used to investigate the degradation of mortar samples made with a diverse range of material in an environment prone to thaumasite sulfate attack. The collected data will provide valuable insights into the precipitation, localization and characterization of potential thaumasite with or without ettringite precipitation; thus selecting more efficient degradation indicators corresponding to thaumasite formation. This is achieved by using an innovative method aiming to better represent real-world conditions found in deep foundations: sulfates were incorporated directly into the mixing water. Prismatic mortar samples were immerged in sodium sulfate solution at 5 °C for 18 months. The degradation of the samples was monitored by mass and length measurements. After 28 weeks of test, the samples were characterized by Scanning electron microscopy coupled with energy-dispersive X-ray spectroscopy (SEM-EDX) and X-ray diffraction (XRD). Mortar samples were also kept in sulfate solution at 20 °C to compare the effect of temperature on the degradation.

This method aims to offer a more accurate and comprehensive assessment of the resistance of cement-based material to thaumasite sulfate attack (TSA) in deep foundation scenarios. Consequently, the initial section of this article is devoted to the development and experimentation of this innovative characterization method. Subsequently, a diverse range of materials were subjected to testing using this method to assess its limitations regarding factors such as C_3A content, the type and proportion of filler, and the influence of various mineral SCMs, including slag, metakaolin, and fly ash. The composition of the mortar samples was selected to represent extreme compositions as the ones limited by standards. Two different types of cement (Cement A, Cement B) were selected. Additionally, the impact of various mineral additions, such as slag, fly ash, metakaolin, and fillers, was explored. Understanding their contribution is crucial for the design of concrete exposed to potential sulfate attacks over its service life.

2. Experimental procedure

2.1. Standard test methods and derived protocol for deep foundations

The difference between the derived protocol for deep foundations and the Procedure B (CSA A3004-C8) are given in Table 1. The reference mortar compositions are derived from ASTM C1012, with a water-to-cement ratio E/C of 0.485. Ottawa sand of type 20–30

was used in accordance to ASTM C778 [19]. It is manufactured to pass through a No. 20 (850 μm) sieve and be retained on a No. 30 (600 μm) sieve. This specially graded sand for ASTM tests consists of naturally rounded silica sands that are nearly pure quartz, mined from the Ottawa, Illinois area. The bar dimensions were selected in accordance with the requirements of Specification C490 [20]. The high slenderness minimizes end effects and allows uniform length change along the specimen, making the measurement more reliable. The higher the length, the lower the relative uncertainty on measured strains. The dimensions of cross section (25 ×25 mm^2) allow reducing the response time of the test while keeping a representative volume of material, considering the maximum aggregate size. Previous research has shown that the response time depends of the dimensions of cross section, but the degradation mechanism induced by external sulfate attack does not change [21]. To account for the absence of specific curing in deep foundation concretes, which are in direct contact with groundwater after casting, the specimens were exposed to an external sulfate solution immediately after demolding at 24 h without any preconditioning. This differs from ASTM C1012 standard, which calls for exposure to a sulfate solution only after the concrete achieves a minimum strength following a minimum 24-hour curing at 35°C ± 3°C. This requirement likely reflects specific criteria related to formwork removal and curing, as applicable to minimum strength standards in the United States.

In the proposed protocol, the water used for batching had the same sodium sulfate concentration as the external exposure. This approach was adopted to reflect real conditions, as fresh concrete cast directly against soil is susceptible to groundwater infiltration, which can introduce sulfate into the material. The sulfate concentration of 4500 g/L (corresponding to 6650 g/L of sodium sulfate) was selected within the 3000–6000 g/L range specified for the XA3 exposure class according to NF EN 206 [22]. This level was chosen to represent aggressive exposure while avoiding the excessively severe conditions associated with CSA A3004-C8, Procedure B. Two testing temperatures, 5°C and 23°C, were chosen to account for different environmental conditions and their influence on sulfate attack. Thaumasite cannot precipitate at 23 ° C; at this temperature ettringite and/or gypsum are the main products of external sulfate attack. The samples were tested following the protocol specified in Table 1.

The formation of thaumasite depends on several conditions that this test endeavours to reproduce. According to Crammond [1], these conditions are as follow: a temperature lower than 5 °C, high and constant relative humidity and a significant supply of sulfate and carbonate ions. The test temperature was set at 5 °C and the samples were completely immerged in a sulfate solution. The sulfate concentration wa in the range of European exposure class XA3 and significantly lower than the 50,000 mg/L concentration specified in ASTM C1012 or the Canadian variation. It is noteworthy that the sulfate concentration directly influences the stability of sulfate-rich phases and the phenomenology of sulfate attack [23,24]. The carbonate source comes from the samples themselves. Samples containing carbonate-rich fillers are significantly affected by TSA [25]. Calcium carbonate (limestone) and calcium magnesium carbonate (dolomite) were used as a source of carbonates.

To ensure experimental reliability, all measurements were conducted in a climate room maintained at 20 °C. Each prism was first removed from the sulfate solution and placed in the comparator for reading and recording of the measurement. Afterward, the prism was returned to the sulfate solution, and the base hole of the comparator was cleaned. For each prism, the length indicated by the comparator was read and recorded along with the length of the reference bar. The comparator used met the precision requirements specified in the ASTM standard. The base hole of the comparator, into which the measuring gauge penetrates at the bottom of the prism, was cleaned before each measurement.

The temperature was carefully controlled, with an allowed tolerance of ±2–3 °C for the target temperatures of 5 °C and 23 °C. Measurements were performed on six prisms per mix. The attack solution was prepared at each renewal, and the pH was measured before use. The solution was discarded if the pH was not within the range of 6.0–8.0.

A precision test was conducted to observe the dispersion of measurements during repeated testing on identical mixes, to determine the repeatability limit of the study. 21 mixtures were produced with the same composition and under the same conditions, with 6

Table 1
Comparison between the standard method and new proposed protocol.

Item	New protocol	CSA A3004-C8, Procedure B
Sodium sulfate, concentration	6650 mg/L	50000 mg/L
Exposure to sulfate	External and batching water	External
Time before demolding	23.5 ± 0.5 h @ 23 ± 3 °C	23.5 ± 0.5 h @ 35 ± 3 °C
Initial curing	-	24 h in saturated lime water @ 23 °C
Immersion in sulfate solution at 5°C	After 23.5 ± 0.5 h, t_0	Compressive strength Rc ≥ 20 MPa, t_0
Sand	Sand ASTM C778 20–30 Ottawa	ASTM C778 graded Ottawa sand and specified in ASTM1012
Slump test	180 ± 20 mm	280 ± 15 mm
Mortars	- Derived from ASTMC109, one part by mass of cement, 2.75 part of sand and water/binder= 0.485. Water/Binder ratio remains unchanged when incorporating additions. - Limestone powder is considered as addition - Sodium sulfate in mixing water - 25 × 25 x 285 mm prisms	- ASTMC109, one part by mass of cement, 2.75 part of sand and, water/cement W/C = 0.485. C= ashes, slag. W/C can be adjusted to reach the desired slump level - 25 × 25 x 285 mm prisms
Renewal of sulfate solution	Once every 15 days	1,2,3,4,8,13, 15 weeks and then 4, 6, 9, 12 et 18 months

prisms for each mixture. The test was conducted on mixture AC35 (Table 2).

The measurements on these prisms followed the same procedure as the rest of the study and they were taken at defined time intervals: 1 week, 2 weeks, 3 weeks, 8 weeks, 13 weeks, 15 weeks, 4 months, 6 months, 9 months, 12 months, and 18 months. The formula used to determine the repeatability limit, and therefore the uncertainty for prism measurements, is given in Eq. 1.

$$\textit{Repeatability limit} = 1.96 \times \sqrt{2 \times \sigma^2} \quad (1)$$

where σ represents the standard deviation.

By grouping the results for each measurement according to the measurement time, the measurement uncertainties were obtained for each week (Table 2).

2.2. Materials and test procedures

2.2.1. Materials

The used sand was Ottawa sand the 20–30 in accordance with the ASTM C778 standard. Two Portland cements of two different types were used in the mortar preparation. Cement A was cement CEM I 52.5 N from Martres, with a C_3A content of 9.9 %, and Cement B was CEM I 52.5 N from Val D'Azergues, with a low C_3A content ($C_3A<3$ %). Table 2 presents gives the compositions of the cements. The limestone filler was sourced from natural Calcium Carbonate of Entrains, France. The second one came from Sala, Sweden; it included Dolomite, a mineral phase containing both calcium and magnesium carbonate. Detailed information about the chemical compositions can be found in Table 2. Three mineral additions were examined: metakaolin, fly ash, and slag. The metakaolin was produced from the flash calcination of kaolinic sandy clays of Bretou, France. Fly ash was produced in Hornaing, France. Slag was ground granulated blastfurnace slag (GGBFS) from Dunkirk, France. Detailed information about the compositions of these additions is provided in Table 2.

2.2.2. Compositions

Various compositions were considered for each type of cement. These compositions were designed by substituting a portion of the cement (in mass) with one or more additions. According to the Canadian Standards Association CSA A3000 [26], binary blended Portland-limestone cements (PLC) must have at least 25 % fly ash, 40 % slag, and 15 % metakaolin by mass of the binder. The chosen proportions were equal of higher than these requirements: 25 % fly ash, 50 % slag, and 25 % metakaolin. Specific details regarding these compositions are presented in Table 3.

2.2.3. Testing methods

The performance of specimens in sulfate environment was evaluated at 5°C and 23°C. The specimens were kept in their molds at room temperature (23 ± 3 °C) for 24 h and then demolded. Subsequently, mortar specimens were fully immersed in sodium sulfate solution within plastic container for a period of 18 months. The volumetric ratio of sulfate solution to mortar bars was maintained at 4:1. The sulfate solution in the container was renewed every 15 days, as indicated in Table 1. Throughout the experiment, mass, length, and visual appearance of the mortar prisms were monitored. These properties were assessed at various curing ages during the experiment. The measurements were recorded at specific times after samples preparation: 24 h (M_i, L_i), and subsequently at 1, 2, 3, 4, 8, 13, and 15 weeks, then 4, 6, 9, 12, and 18 months, in accordance with the ASTM C1012 standard [18].

The mass variation of each mortar prism was calculated as follows:

$$\Delta m \quad (\%) = \frac{M_t - M_i}{M_i} \times *100 \quad (\%) \quad (2)$$

where M_i is the initial mass of prism and M_t is the mass of prism at measurement time (t).

The length variation resulting from expansion or shrinkage during sulfate exposure was monitored by using length comparator according to ASTM C1012 standard. The length variation of mortar prism was calculated as follows:

Table 2
Repeatability test results.

Time (weeks)	Average (%)	Repeatability standard variation (%)	Repeatability limit (%)
1 weeks	0.0003	0.0019	0.0056
2 weeks	0.0003	0.0020	0.0060
3 weeks	0.0002	0.0021	0.0062
4 weeks	−0.0003	0.0024	0.0078
8 weeks	0.0034	0.0021	0.0065
13 weeks	0.0072	0.0028	0.0099
15 weeks	0.0086	0.0031	0.0102
4 Months	0.0087	0.0028	0.0083
6 Months	0.0180	0.0029	0.0099
9 Months	0.0466	0.0029	0.0100
12 Months	0.0745	0.0064	0.0229
18 Months	0.1724	0.0109	0.0314

Table 3
Chemical and physical composition of materials.

Material	Portland cement		Filler		Additions		
Name (wt%)	**Cement A**	**Cement B**	**Limestone**	**Dolomite**	**Fly Ash**	**Slag**	**Metakaolin**
SiO_2	19.77	20.81		3.6	50	35.1	92.5
Al_2O_3	5.25	3.46		0.6	26	11.1	
Fe_2O_3	2.73	5.05		0.5	8	0.4	
CaO	64.49	64.56	98	30.2	4.5	42.1	0.32
MgO	1.55	0.75		20.6	2	7	0.19
TiO_2	0.24	0.23			0.75	0.8	
SO_3	3.14	2.69			1.1	0.1	
Cl^-	0.01	0.07	0.03		0.04	0.03	0.002
S^{2-}	0.00	0.00	0.02			0.6	
Na_2O	0.25	0.15			0.75	0.21	0.25
K_2O	0.49	0.59			3.5	0.43	
Density (kg/m^3)	3130	3200	2700		2200	2900	
Specific surface area (m^2/g)	3985	3870	5950			4200	

Table 4
Proportions of cement and mineral additions of studied binders.

Cement	Name	Filler		Additions		
		Limestone	**Dolomite**	**Fly Ash**	**Slag**	**Metakaolin**
Cement A	A	-	-	-	-	-
	AC15	0.15	-	-	-	-
	AC25	0.25	-	-	-	-
	AC35	0.35	-	-	-	-
	AD15	-	0.15	-	-	-
	AD25	-	0.25	-	-	-
	AD35	-	0.35	-	-	-
	AF25		-	0.25	-	-
	AC15F25	0.15	-	0.25	-	-
	AC25F25	0.25	-	0.25	-	-
	AC35F25	0.35	-	0.25	-	-
	AD15F25	-	0.15	0.25	-	-
	AD25F25	-	0.25	0.25	-	-
	AD35F25	-	0.35	0.25	-	-
	AS50	-	-	-	0.5	-
	AC15S50	0.15	-	-	0.5	-
	AC25S50	0.25	-	-	0.5	-
	AC35S50	0.35	-	-	0.5	-
	AD15S50	-	0.15	-	0.5	-
	AD25S50	-	0.25	-	0.5	-
	AD35S50	-	0.35	-	0.5	-
	AM25	-	-	-	-	0.25
	AC15M25	0.15	-	-	-	0.25
	AC25M25	0.25	-	-	-	0.25
	AC35M25	0.35	-	-	-	0.25
Cement B	B	-	-	-	-	-
	BC15	0.15	-	-	-	-
	BC25	0.25	-	-	-	-
	BC35	0.35	-	-	-	-
	BM25	-	-	-	-	0.25
	BC15M25	0.15	-	-	-	0.25
	BC25M25	-	-	-	-	0.25
	BC35M25	-	-	-	-	0.25
	BF25	-	-	0.25	-	-
	BC15F25	0.15	-	0.25	-	-
	BC25F25	0.25	-	0.25	-	-
	BC35F25	0.35	-	0.25	-	-
	BS50	_	-	-	0.5	-
	BC15S50	0.15	-	-	0.5	-
	BC25S50	0.25	-	-	0.5	-
	BC35S50	0.35	-	-	0.5	-

$$\Delta L(\%) = \frac{L_t - L_i}{L_i} \times *100 \quad (\%) \tag{3}$$

where L_i is the initial length of prism and L_t is the length of prism at time (t).

Tests for compressive strength were performed on three chosen mixtures (AC25, AC35, and AD25F25) that demonstrated high level of degradation due to external sulfate attack. Mixtures were cast in cylindrical molds with a diameter of 40 mm and a height of 80 mm, i.e. a shape and slenderness complying with NF EN 12390–1 standards [27]. Test were performed on samples exposed to sulfate at both 5°C and 23°C, after 3 months when the first signs of degradation were visible on samples. Tests were also performed on control samples immersed in demineralized water at 5°C and 20°C. The compressive strength was evaluated using a loading rate of 1.9 kN/s until failure [28],with three samples tested for each mixture. At microscopic level, X-ray diffraction (XRD) was used to identify and characterize crystalline phases qualitatively in these mixtures after 7 months for two samples AC35 and AD25F25. XRD spectrum of mortar samples was obtained using a BRUKER - D8 Advance on powdered samples taken from crushed prisms. The operating voltage and current were set at 40.0 kV and 40.0 mA. This diffractometer model is equipped with a copper anode tube (Cu-Kα: $\lambda = 1.54060$ Å). Disoriented powder diffractograms were recorded between 7°2θ and 40°2θ, with a pitch of 0.01°2θ.

Scanning electron microscopy coupled with energy-dispersive X-ray spectroscopy (SEM-EDX) analysis was conducted to investigate the presence of reaction products and microstructural alterations due to sulfate exposure after 7 months. The EDX component of the analysis provides information about the elemental composition of the samples. To perform the SEM and EDX analyses, small sections of mortars were extracted from various sets of mortar prisms. These two tests were used to investigate the formation of reaction products under sulfate exposure at 5°C. However, they were selectively performed on specific mixtures (AC35 and AD25F25).

It is important to note that macroscopic scale tests (mass variation, length variation, and compressive strength) were conducted on all mixtures tested at both 5°C and 23°C. The purpose of these tests was to highlight the differences in performance at 5°C and 23°C among the various mixtures. Microscopic scale tests were conducted exclusively on the samples degraded at 5°C. The reactions and

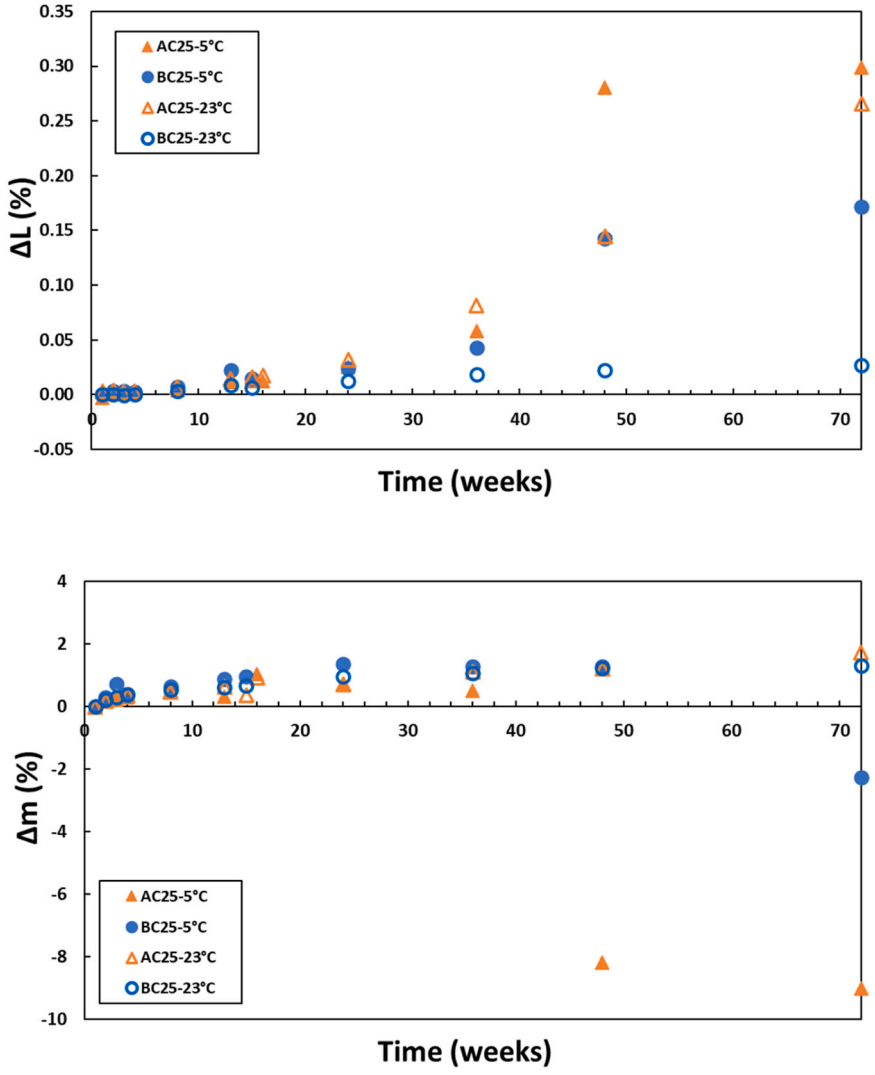

Fig. 1. Effect of C_3A content on mass and length variations at 5°C and 23°C.

mechanisms at 23°C are well-documented and extensively studied in the literature.

3. Results and discussion

3.1. Influence of binder composition

3.1.1. Effect of C_3A and filler contents

In this section, the effect of e C_3A (as part of the cement clinker) and filler content was investigated. These two binder components have a crucial role in the external sulfate attack at 20 °C or 5 °C. Hydrated C_3A represents the main source of aluminates for the precipitation of ettringite and fillers provide carbonates essential for the precipitation of thaumasite.

Fig. 1 presents mass and length variations, at both 5°C and 23°C. At 23°C, the sulfate-resistant cement B (BC25–23°C) led to significantly lower expansion than cement A (AC25–23°C), with changes not exceeding 0.1 %. Ettringite formation is favored at higher aluminate content and subsequently increases the potential for thaumasite formation via the indirect route as explained earlier [29]. However, it is noteworthy to mention that even the samples BC25–5°C made with the sulfate-resistant cement B experienced some deterioration when exposed to 5 °C, with variations exceeding 0.1 %, thus exhibiting a non-sulfate resistant behavior.

The samples prepared with cement B had a lower mass loss than those made with cement A (AC25–5 °C) even in colder

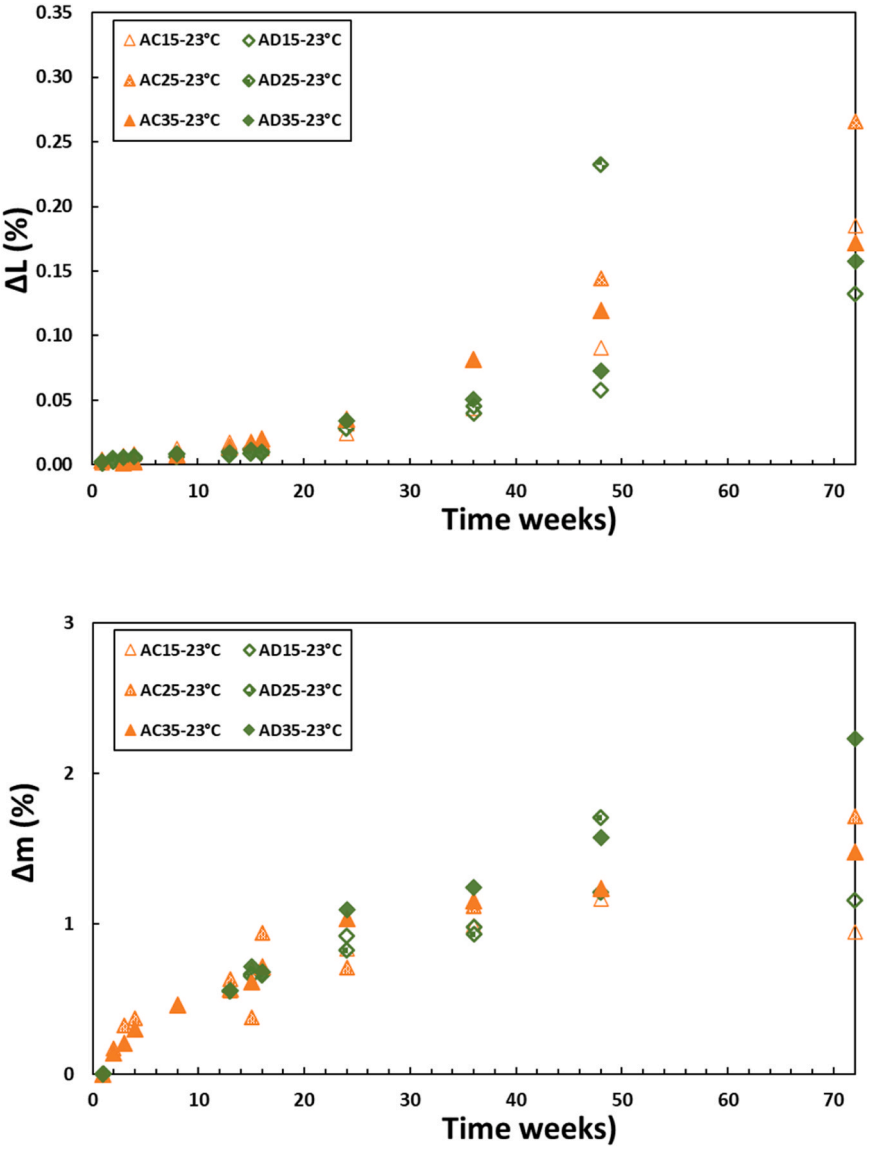

Fig. 2. Effect of the proportion and type of filler on mass and length variations at 23 °C.

environments. The increased vulnerability of cement B to sulfate attack at 5 °C can be attributed to its significant C_3S content, which results in a high amount of portlandite which leaching results in the solubilization of calcium ions. Those solubilized calcium ions can thus react with sulfate from the solution and the aluminates, from C_3A, to form ettringite then leading to the formation of thaumasite. According to the literature Thaumasite formation comes from the reaction of carbonate with C-S-H or from the reaction of ettringite with C-S-H. In both cases, the precipition of thaumasite involves the degradation of C-S-H. Consequently it affects the cement matrix ability to oppose to crystallization pressure induced by the formation of sulfate rich-phases. This could explain the higher expansion (in length) of BC-5 °C than BC25–23 °C. Those results show that while it is known that ettringite formation may be required for thaumasite precipitation, thaumasite precipitation equally affects the degradation caused by ettringite. In the meantime, the mass variation of sample AC25–5 °C negatively follows the length variation. There is a significant drop in mass corresponding to an important increase in length, suggesting that they can be related to the same phenomenon. However, for BC25–5°C, the mass loss happened after the important increase in length and resulted in the breaking of the sample.

Fig. 2 illustrates the impact of filler type and proportion on sulfate attack at 23 °C. Increasing the filler proportion to 25 % and 35 % resulted in more significant expansions. When the filler content is low (around 5 %), the porosity decrease. Finer porosity slows down the progression of sulfates in the material and therefore limits the possibility of ettringite formation. But from a proportion of 25 % filler, the porosity will increase accordingly [30]. It is noteworthy that the length variations exceeded the accepted expansion limit of 0.1 %. From the experimental results, the type of filler does not appear to influence the rate of sulfate attack, which aligns with previous research findings [31]. Both limestone and dolomite fillers did not directly participate in the sulfate attack process at 23 °C.

Fig. 3 illustrates the relationship between the increase in filler proportion and the progressive deterioration of samples at 5°C. When there is an abundance of carbonates or bicarbonates within the cementitious matrix, combined with sufficient moisture and low temperature, thaumasite can readily form [32]. The presence of monocarbonate originating from limestone, in addition to ettringite, serves as initiators for TSA.The susceptibility of concrete to TSA is heightened when the mixtures contain elevated levels of finely divided carbonate, like limestone filler, exceeding 10 % of the binder mass as reported in [33]. Even if the carbonate content is not relatively high, the presence of these compounds can contribute to the initiation of TSA [30].

The type of filler had a notable impact on their resistance to TSA. Fig. 3 shows that the length variations were higher with limestone filler than dolomite. However, mass variations were lower and the significant mass decrease appeared later. The observed variations are logical as the decrease in sample mass, or its deterioration, leads to material loss, consequently countering the length expansion. These evolutions can also be attributed to the contribution of magnesium attack processes. The magnesium from dolomite react with portlandite to form magnesium hydroxide (brucite, $Mg(OH)_2$) and gypsum [34]. The relatively low solubility of brucite induces a substantial decrease in pH, thereby destabilizing the C–S–H (Calcium Silicate Hydrate) phase. Once all the portlandite is consumed, it ultimately results in the formation of magnesium silicate hydrate (M–S–H) or amorphous hydrous silica (SiO_2·aq), both of which a lack of binding properties [31,35,36]. The mass variation increased with dolomite content, which was not systematically observed for limestone. Finally, cement paste is transformed into a non-cohesive mass leading to the loss of pieces of material [28,32,37].

The compressive strength of the control specimens at 20°C and the specimens exposed to sulfate solution during 12 weeks is presented in Fig. 4, with two different curing conditions. Notably, all specimens tested at 5°C exhibited a decrease in compressive strength compared to those tested at 23 °C. This difference was not significant for AC25 and AC35. The mixtures containing dolomite and fly ash experienced a significant decrease in compressive strength of 37 % respectively at 5°C. It can be explained by the slow pozzolanic reaction of fly ash at low temperatures, which influences the development of strength [38]. This reduction may reduce the resistance of fly ash–based mixtures to sulfate attack. The differences in compressive strength variations between the exposed

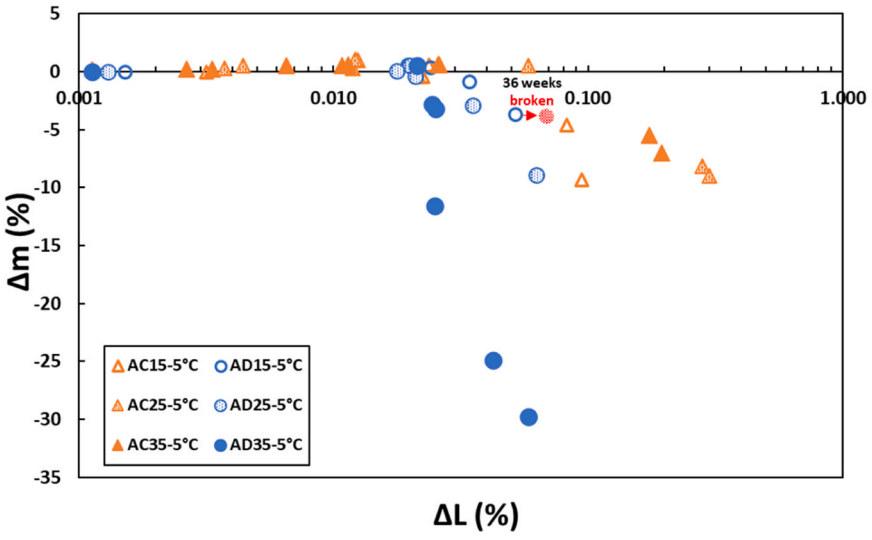

Fig. 3. Effect of the proportion and type of filler on mass and length variations at 5 °C.

specimens and the control specimens was not significant after 12 weeks at both 5 °C and 23 °C.

Fig. 5 displays the visual observations of mortar specimens at different exposure times at both 5 °C and 23°C. The specimens exposed at 23 °C did not show observable signs of surface degradation during the entire immersion period. Ettringite precipitation mainly affect the heart of the sample while leaving the outside part intact [39]. On the other hand, the specimens exposed at 5°C exhibited visible surface deterioration, resulting in the loss of cohesion and part of material. The deterioration of the specimens exposed at 5 °C was more pronounced compared to those exposed at 23 °C [40]. The degradation process continued over time, resulting in the fracture of specimen AD15F25 after 24 weeks and specimen AD25F25 after 36 weeks at 5 °C. However, this fracture was not observed at 23 °C. These observations are compatible with the mechanism of degradation specific to thaumasite formation and the replacement of calcium compounds (portlandite and C-S-H) with magnesium non cohesive compounds (brucite and M-S-H) [41].

3.1.2. *Effect of mineral additions*

A series of experiments were conducted to investigate the impact of the main mineral addition on materials performance, with the replacement of cement with slag, metakaolin, and fly ash at 5 °C and 23 °C. The results of these experiments are illustrated in Fig. 6 and Fig. 7. The results obtained at 23 °C consistently show a common trend for the three additions, namely a reduction in mass and length variations for all the ternary binders. This result is in accordance with previous findings reporting that the incorporation of fly ash, slag and metakaolin can mitigate the expansion and damage caused by sulfate attack [25,42]. The enhancement of sulfate resistance in concrete due to mineral additions arises from the initiation of pozzolanic reactions, which deplete calcium hydroxide. Additionally, substituting cement with mineral additions results in a reduction of the clinker part thus a reduction of reactive aluminates from C_3A within the system that have been extensively demonstrated as the primary source of aluminates for the formation of ettringite [34,43,44]. The inclusion of mineral additions in mixtures also results in decreased diffusivity, preventing harmful penetration of sulfate ions [15,42].

At a temperature of 5 °C, similar findings as 23 °C were observed when incorporating slag and metakaolin. The replacement of cement with both mineral additions resulted in a reduction in mass and length variations. The replacement of Portland cement by pozzolanic additions induce a reduction in calcium hydroxide and C_3A contents within the cementitious matrix, limiting the formation of thaumasite and improving the resistance of mixtures against TSA [25].

The incorporation of fly ash as a mineral addition did not yield favorable outcomes at 5 °C. Unlike metakaolin and slag, which exhibit both pozzolanic and binding properties, fly ash primarily contributes to the pozzolanic reaction [45]. Fly ash exhibits a relatively slow pozzolanic reaction, and its reactivity is influenced by temperature variations [38], as confirmed by the results displayed on Fig. 4. Previous research has revealed that increasing the temperature from 7 to 23 °C shifts the onset of the pozzolanic reaction from 90 days to 7 days [46]. Consequently, at 5 °C, the interaction between fly ash and calcium hydroxide to produce secondary C-S-H gels, which reinforce the hydrated cement matrix, is limited. As results, the resistance to crystallization expansion due to ettringite formation promoted by the presence of portlandite is lower [47]. Consequently, mixtures containing fly ash were more susceptible to deterioration caused by TSA when compared to those containing slag and metakaolin.

3.1.3. *Discussion*

Fig. 8 provides an overview of the length and mass evolution as a function of the percentage of filler for all the mixtures tested during this study after 12 months. The initial presumption was that the threshold values of length that could be linked to a pathology are 0.05 % at 6 months and 0.1 % at 12 months as reported in ASTM C1012 [19]. The results revealed that with an increasing

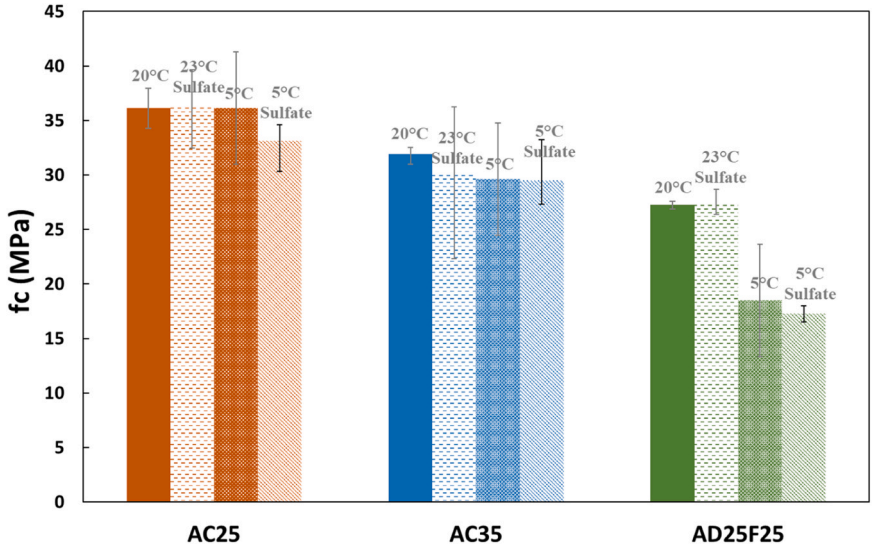

Fig. 4. Compressive strength of mortars at 23 °C and 5 °C after 12 weeks in sulfate solution and control specimens.

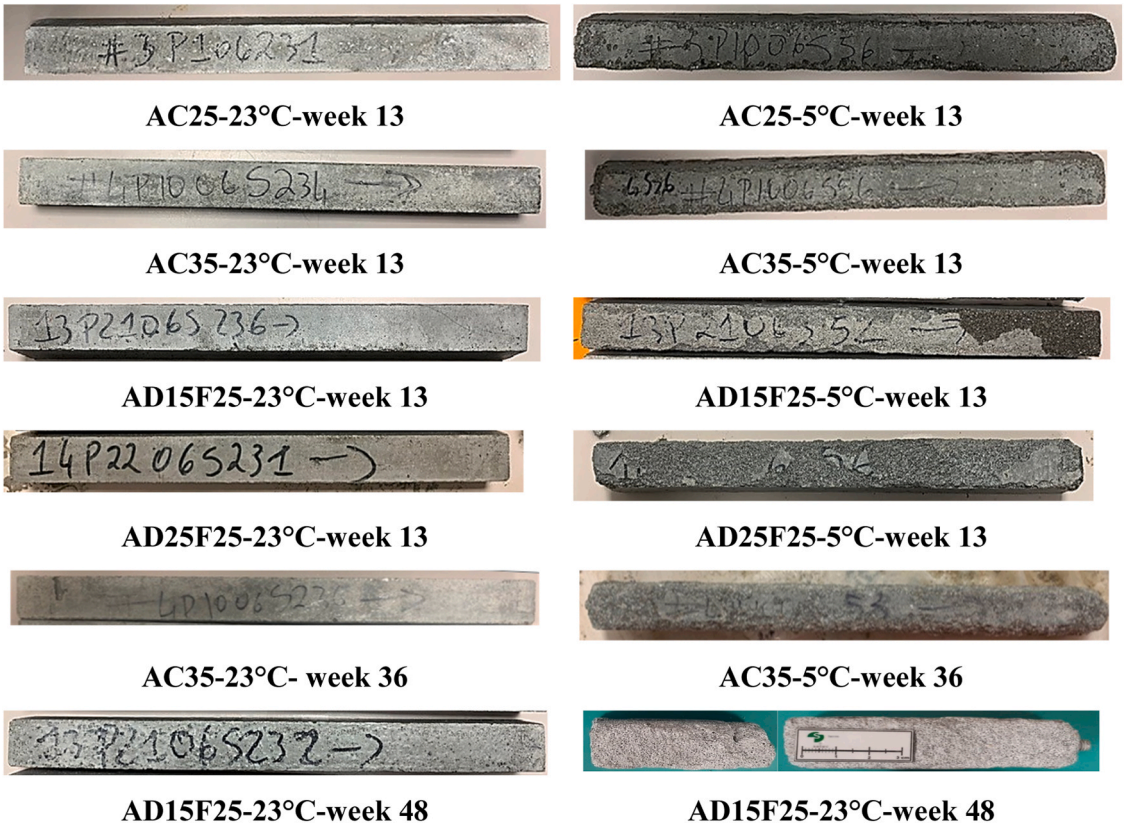

Fig. 5. Visual degradation of different specimens after 13 weeks at 5 °C and 23 °C.

proportion of filler, the resistance to TSA was reduced. Incorporating filler content of 15 % or more into mixtures A and B led to higher length variation and mass loss. This pattern was consistent for both limestone and dolomite fillers. Several mixtures lead to significant mass loss or deterioration consistent with TSA. AF25, AD15, and BC35 specimens broke within 12 months; a red cross on the dashed line representing the length threshold value marked them. AC15, AC25, AC35, and AC15F25 specimens exhibited failure in terms of the length threshold ($\Delta L > 0.1$ %) and displayed higher mass loss ($\Delta m > 6$ %). Conversely, the expansion of AD25 and AD35 specimens did not exceed the length variation threshold but they experienced high mass loss ($\Delta m = -25$ % and -29.7 % respectively). Therefore, relying solely on the TSA length threshold of 0.1 % to assess the resistance at 5°C seems insufficient. The length limit set by the standards in sulfate attack condition is related to expansion caused by ettringite formation. However, TSA also induces the formation of thaumasite which involves a loss of binding phases, leading to a significant mass loss as shown in this study. In agreement with experimental results and TSA phenomenology, there is a need to establish a threshold for mass loss to account for thaumasite formation and evaluate the resistance to TSA effectively.

For instance, mixtures like BC35F25 exhibited a relatively lower mass loss of -1.25 % compared with mixture AC35, which showed a higher mass loss of -6 %. The visible degradation of mixture AC35 compared to BC35F25 confirmed the classification of these two mixtures into distinct categories. However, intermediate time points should be added to capture more variation in mass, and a limit should be proposed for acceptable mass loss.

The filler content plays a pivotal role in influencing the susceptibility of cement-based materials to thaumasite formation and sulfate attack. However, the allowed filler content may depend on the use of mineral additions. The effects of additions (slag, fly ash, and metakaolin) were investigated. The results showed that mineral additions played a crucial role in improving mortar resistance to sulfate and TSA at 23 °C and 5 °C. Metakaolin and slag were more effective, improving the mortar resistance to sulfate attack and TSA, whereas fly ash showed less favorable results, especially at 5 °C. Consequently, the use of a percentage of these additions enables a filler percentage of up to 35 % to be used. The BC35 and AC35 specimens showed significant damage, whereas improved resistance to TSA could be observed when 50 % slag and 25 % metakaolin was added (in BC35S50 and AC35M25, respectively). This significant improvement calls into question the filler percentages allowed in American and French standards, which generally remain close to 0 % even with SCM.

3.2. Degradation mechanism at 5 °C

From the above results, it is clear that a high C_3A content and the presence of carbonates in the form of dolomite or limestone fillers

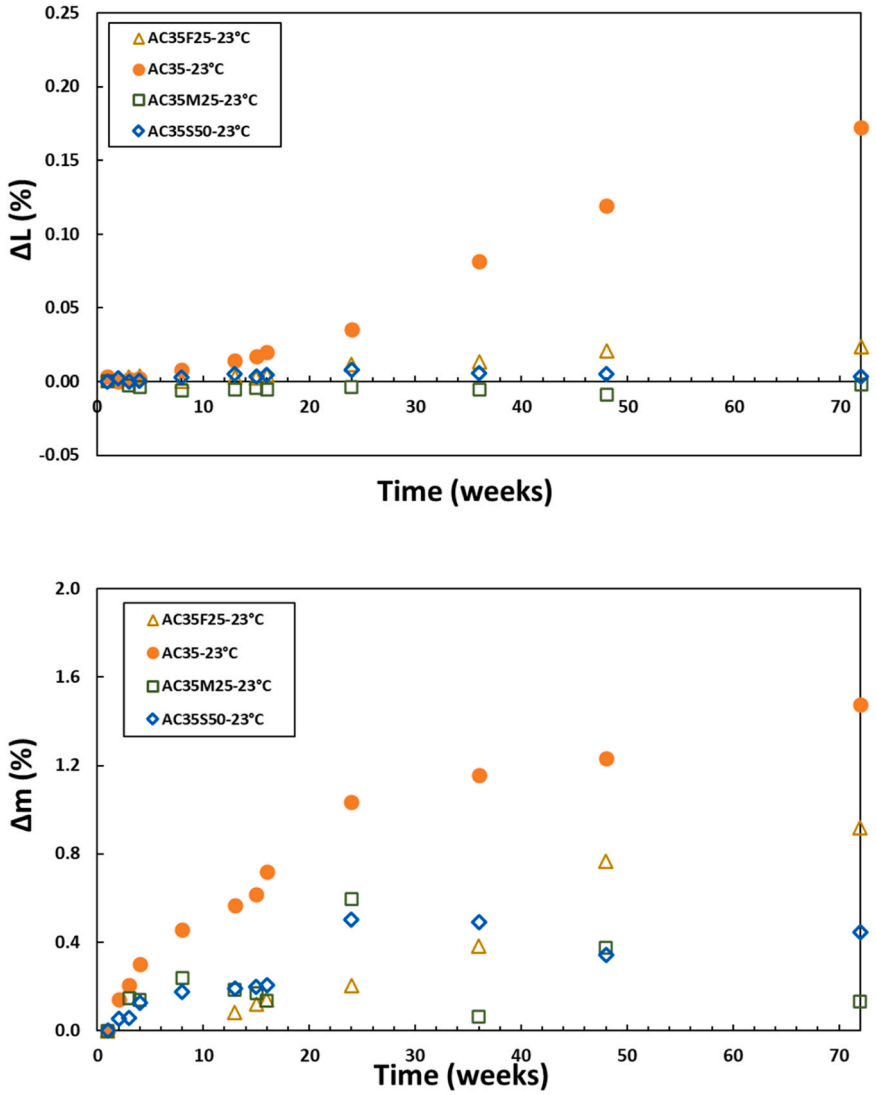

Fig. 6. Effect of mineral additions on mass and length variations at 23 °C.

favor a particular response to sulfate attack. Thaumasite formation could be the cause of the degradation of samples AC25, AC35, AD15F15 and AD25F25 at 5 °C. Microstructural characterization was carried out on the samples to confirm these assumptions.

3.2.1. Mass and length variation

Fig. 9 illustrates the mass and length variations of mortar specimens during sulfate exposure at 5 °C. Initially, all specimens displayed almost identical mass and length variations up to 16 weeks of exposure. However, after this period, the studied mixtures exhibited divergent behaviors.

The AD15F25 mixture showed a mass loss after 24 weeks, accompanied by a relatively low length variation. Subsequently, the failure of the specimen was observed. In contrast, the AD25F25 mixture consistently gained mass until 24 weeks, with a minor length variation. The data for the AD25F25 specimen after 36 weeks could not be obtained due to its fracture. The AC35 specimens experienced a mass decrease after 24 weeks, which occurred before the AC25 mixture. The AC25 mixture showed a mass reduction after 24 weeks, followed by a substantial mass loss of approximately 8 % after 48 weeks. This significant mass loss was accompanied by considerable changes in length, reaching 0.175 % after 36 weeks and 0.28 % after 48 weeks for AC35 and AC25, respectively. These values exceed the limit value of 0.1 % specified in the CSA A3004-C8, Procedure B [25].

The mixtures containing calcium magnesium carbonate fillers and fly ash experienced structural fractures at the same time, even though their mass variations were opposite. This indicate that the precipitation of expansive product can have different macroscopic manifestation. In the case of AD15F15, the break of the samples was certainly preceded by the loss of some material, early-warning of the extreme fragility of the degraded sample. The mixtures containing only limestone filler know a significant drop of their mass

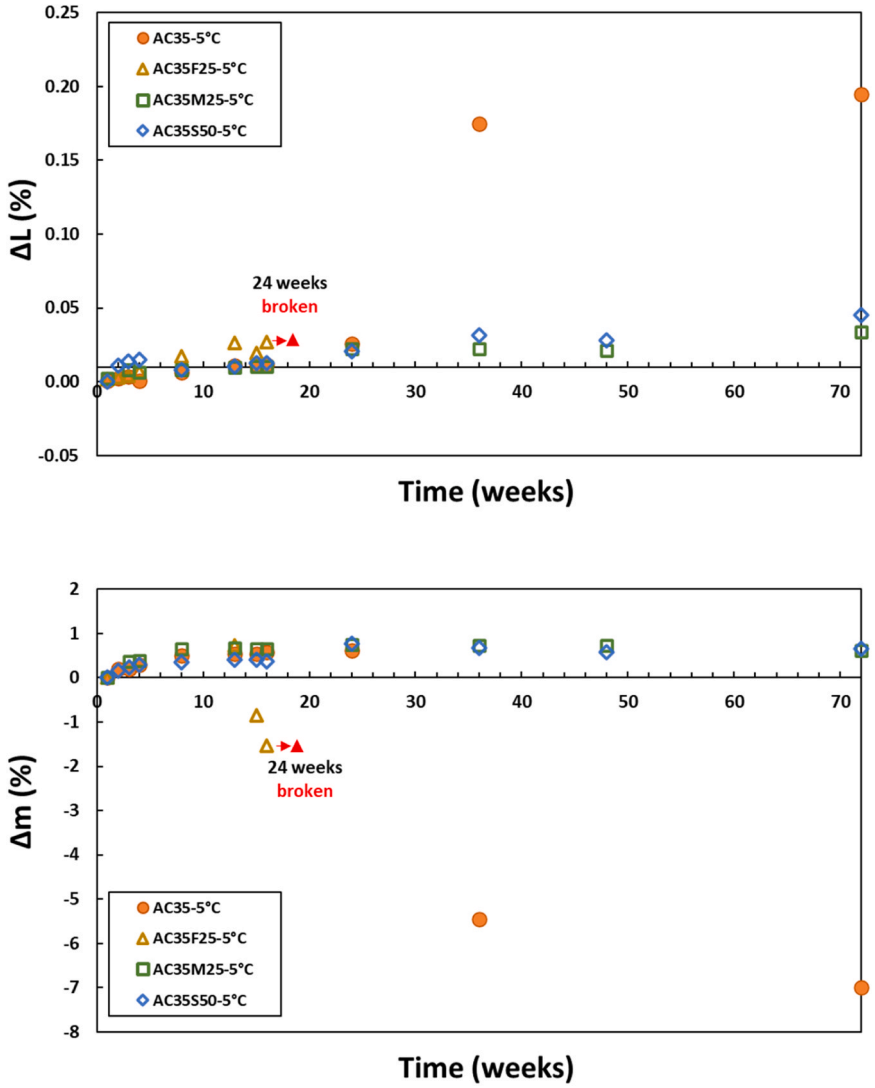

Fig. 7. Effect of mineral additions on mass and length variations at 5 °C.

simultaneously with important increase of their length.

Fig. 10 presents the mass and length variations of all the mortar specimens under sulfate exposure, covering four different mixtures. Each data point on the graph corresponds to the mass and length variation observed at a given age during the exposure period.

The red point with hatching marks denotes the time when the sample experienced failure. A noteworthy observation is the distinct behaviors exhibited by the specimens at two different temperatures, namely 5 °C and 23 °C, for all mixtures. At 23 °C, all mixtures demonstrated a common response characterized by mass gain and specimen expansion. This phenomenon is well-known in non-sulfate resistant cement-based materials under sulfate exposure [45] [39,48]. The expansion of the specimens can often be attributed to the formation of ettringite, a typical reaction product that occurs during external sulfate attack on concrete [49]. According to the theory of crystal growth pressure, crystallization pressures can be generated due to the formation of ettringite in pores smaller than about 100 nm. These stresses may exceed the tensile strength of the binder matrix leading to expansion and structural damage. In larger pores, the presence of large ettringite crystals does not lead to any significant expansion [50]. The presence of gypsum can also contribute to the observed expansion and softening effects [51].

When exposed to sulfate at 5 °C, the mixtures exhibited different behaviors, as mentioned earlier. The specimens showed an increase in length finally coupled with mass loss. This behavior is likely due to the formation of thaumasite, known to cause cracking, spalling, and the formation of non-cohesive mass in concrete [2]. These observations align well with the visual observation presented in Fig. 5. Consequently, the variations in behavior at 23 °C and 5 °C point to different degradation profiles, primarily influenced by the temperature conditions. At 23 °C, the expansion of the samples is simultaneous with their increase in mass indicating the precipitation of ettringite. The samples containing only limestone fillers went through more expansion than the samples containing dolomite and fly ash. It can be caused by the greater clinker content, thus C_3A, content of the AC samples. Moreover, the presence of fly ash is known to

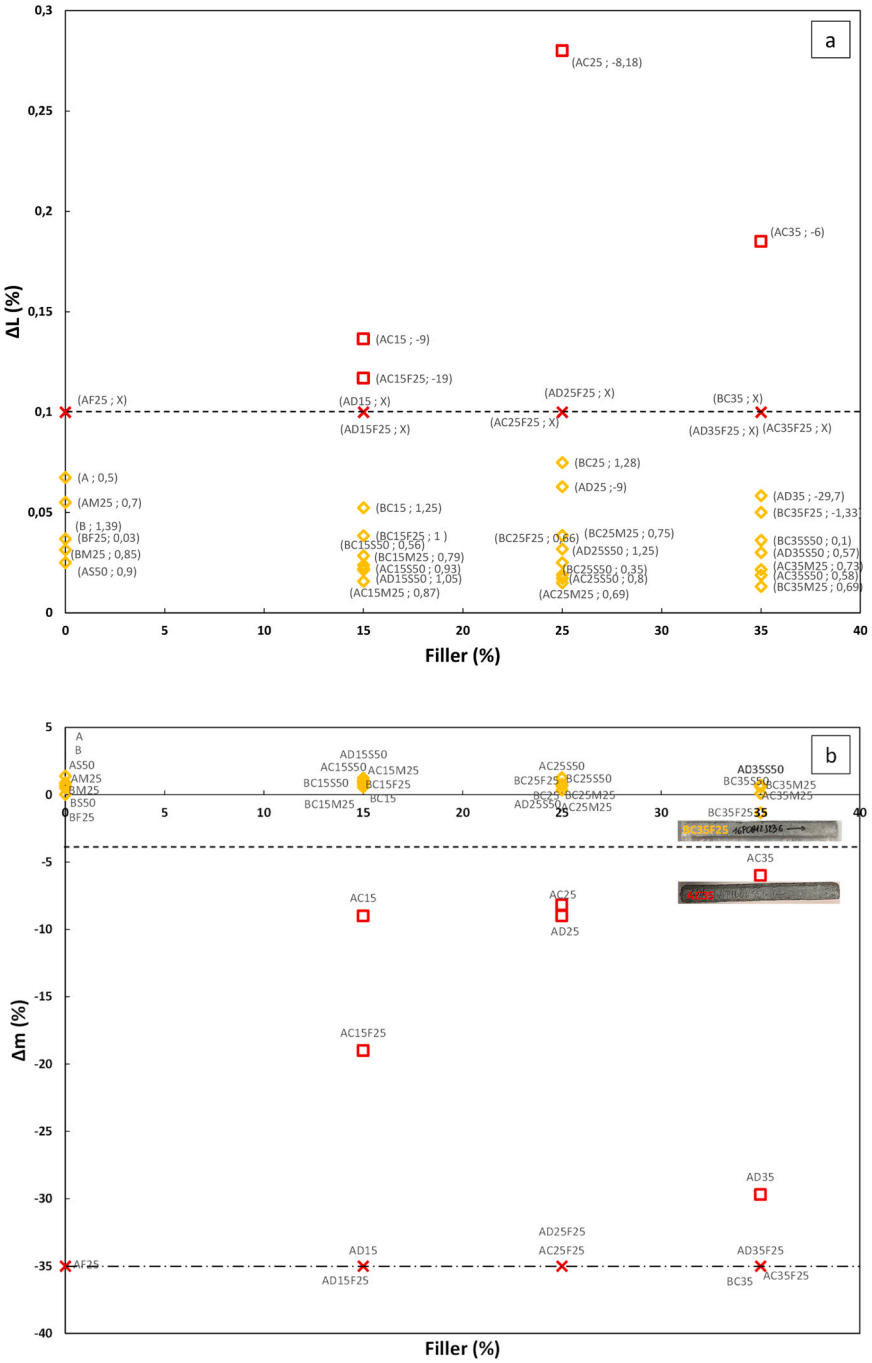

Fig. 8. (a) Variation of length as a function of filler proportions for all studied mixtures; the text refers to (specimen name, % of mass variation) at 5 °C after 12 months. (b) Mass variation Δm as a function of filler proportions.

be responsible for a lower diffusivity of sulfate ions in the cement matrix. At 5 °C, the degradation of all samples was driven by thaumasite precipitation. The presence of magnesium from dolomite also induced the degradation of C-S-H thus contributing to samples embrittlement [52]. The upcoming section explore the XRD and SEM results.

3.2.2. Microstructure evaluation

The SEM analysis was carried out on two types of mortar samples, namely AC35 and AD25F25, stored during 25 weeks at a temperature of 5 °C (Figure). These two samples were selected because they exhibited the most severe degradation under exposure at 5 °C. This makes them representative cases for analyzing the impact of low-temperature attack as well as the influence of mixture

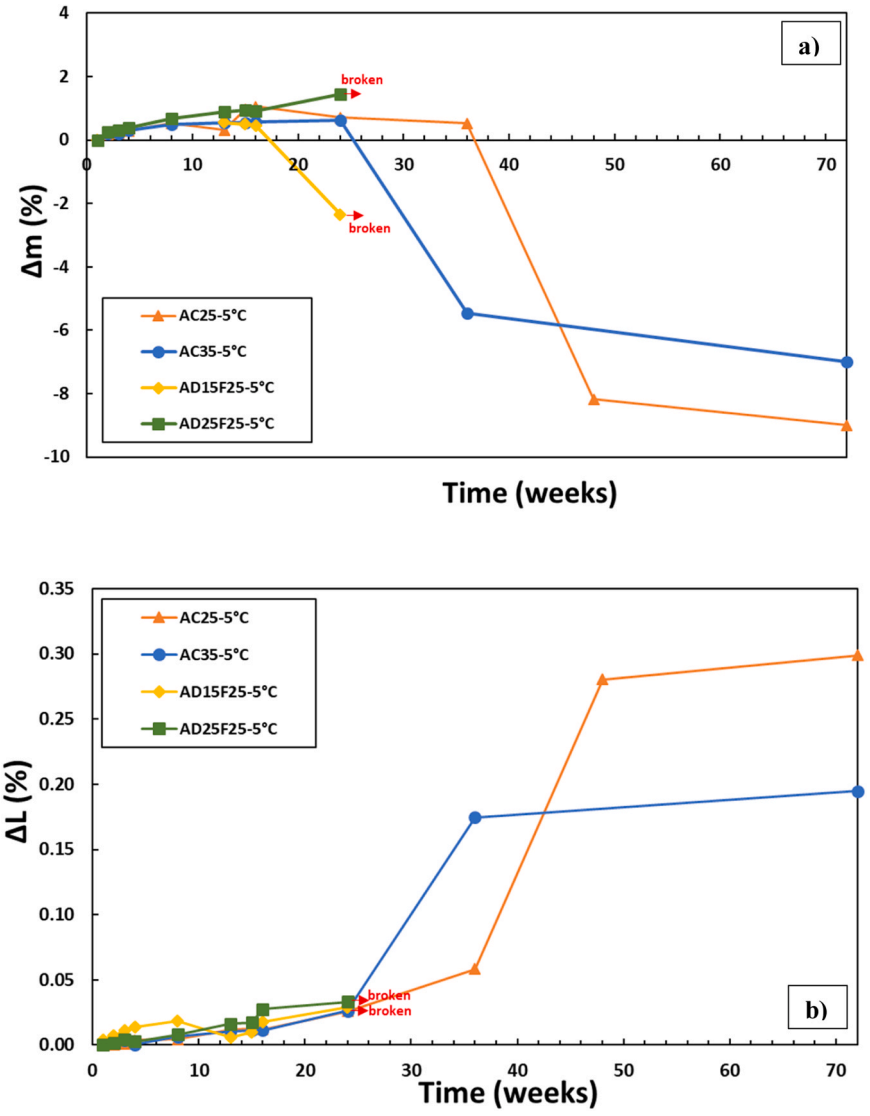

Fig. 9. (a) Mass and (b) length variations of mortar specimens at 5 °C.

composition.

These mortar specimens exhibited a microporous microstructure and demonstrated a robust cohesion between the sand particles and the cement paste. Needle-shaped crystals were identified within the pore matrix of both AC35 and AD25F25 mixtures, suggesting the potential formation of either ettringite or/and thaumasite (Fig. 11. a, b and c). Previous research has indicated that ettringite typically appears as short and stubby crystals, while thaumasite tends to present as acicular crystals [53]. However, the shape of ettringite crystals is greatly influenced by the ionic concentration and the hydration time [54,55]. Nevertheless It is difficult to distinguish between these two morphologies in our study. Notably, in the AD25F25 mixture, unreacted fly ash particles with a more or less spherical shape were observed (Fig. 11. d.)(Fig. 12).

The EDX analysis conducted on AD25F25 revealed peaks corresponding to calcium, sulfur, aluminum, silicon, and oxygen (Fig. 11) that may correspond to ettringite [56]. The EDX also indicated the significant presence of a mineral characterized by elevated levels of silica, calcium, and sulfur (Fig. 11), that can be assumed to be thaumasite. This indicates that ettringite and thaumasite frequently coexisted with each other in the samples. Furthermore, the observation of silicon and aluminum in the EDX spectra of the needle-shaped crystals may suggest the possibility of thaumasite formation through the Woodfordite pathway, in which ettringite reacts with available C-S-H (calcium-silicate-hydrate) and carbonate to generate thaumasite [8].

Mortars specimens were subjected to X-ray diffraction (XRD) analyses to identify different crystalline phases likely to be formed during sulfate exposure (Figure). The XRD profiles revealed distinct peaks corresponding to quartz, calcite, and dolomite. Additionally, the XRD results provided confirmation of the presence of ettringite and gypsum. Peaks corresponding with thaumasite may be present but they are overlapped by peaks of ettringite. It has actually been observed that peaks of ettringite and thaumasite often appeared

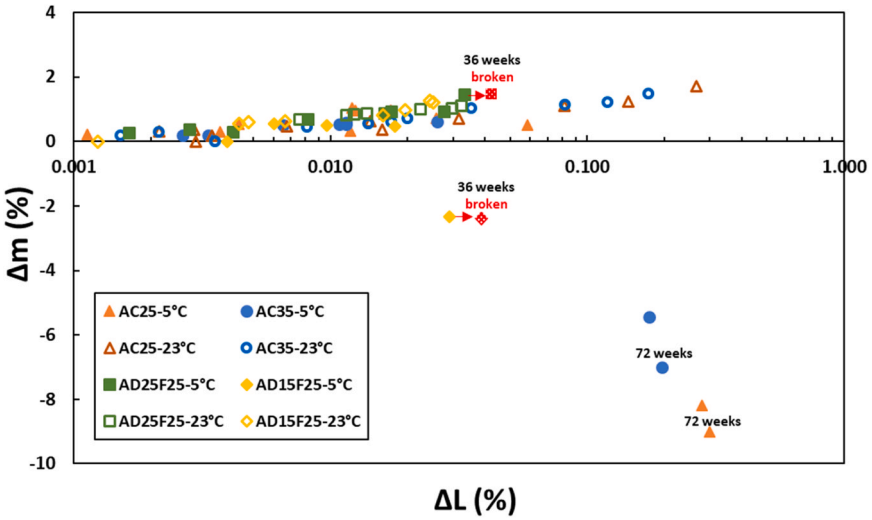

Fig. 10. Mass variation (%) as a function of length variation (%).

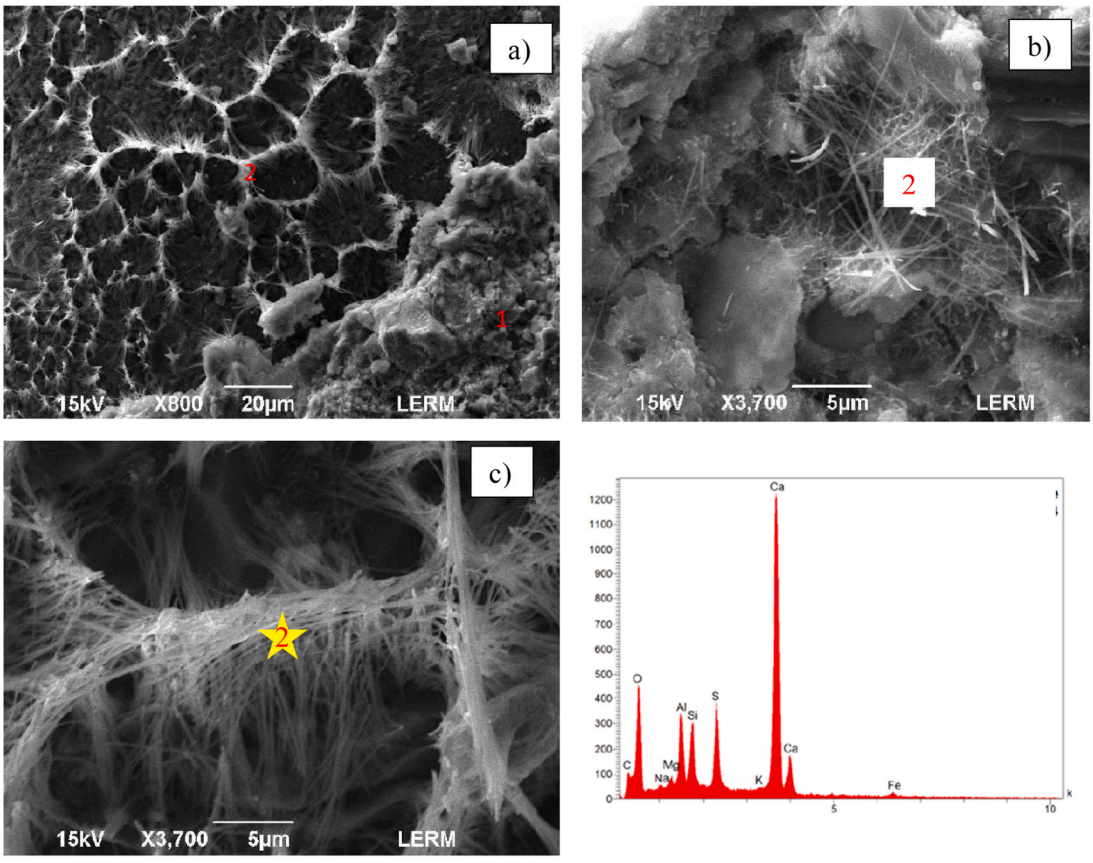

Fig. 11. SEM images of polished specimens after 7 months and EDX analyses; stars show the EDX analysis spots.

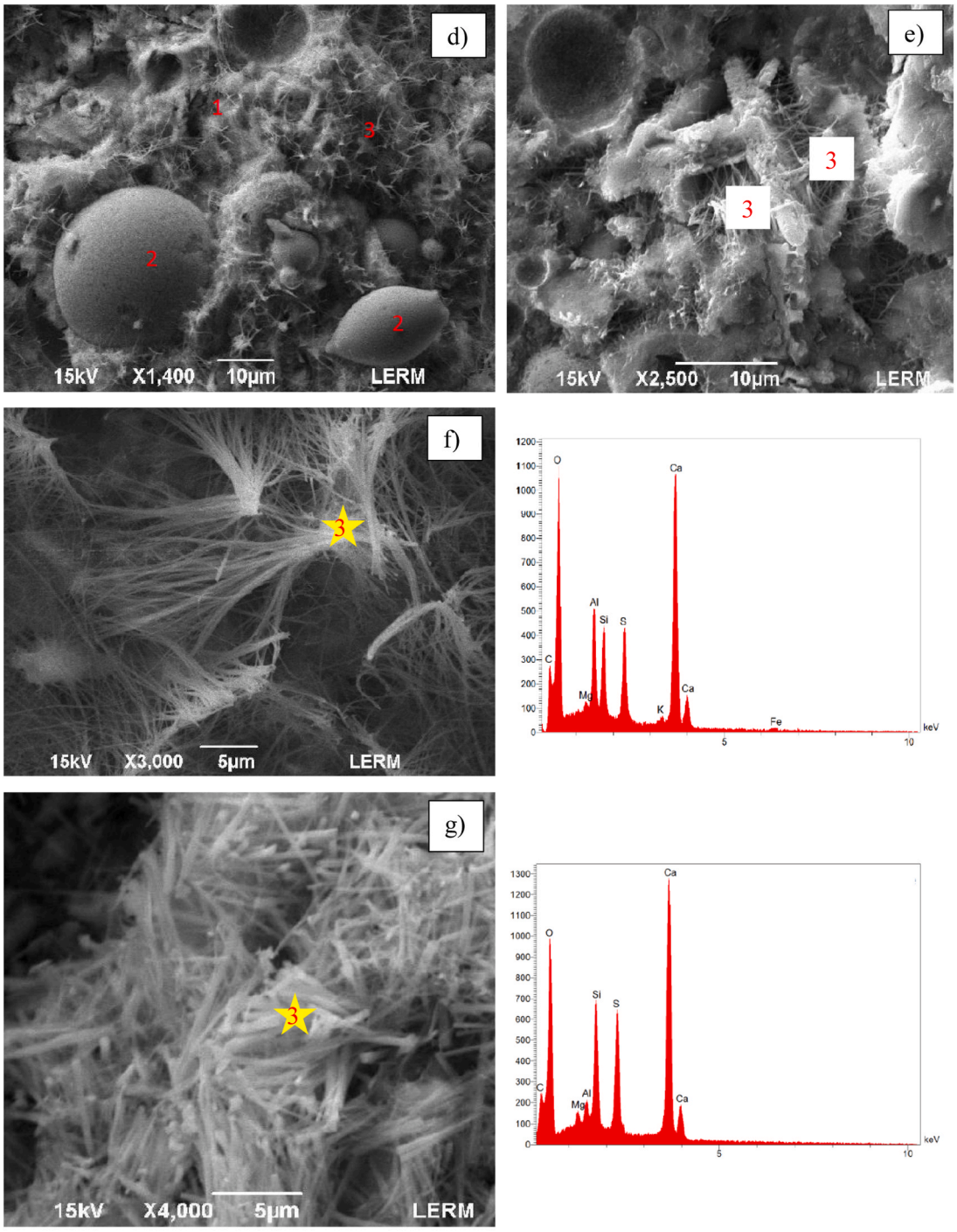

AD25F25-5°C; 1: C-S-H / 2: Fly ash/3: fine needles

Fig. 11. (*continued*).

together [53,57].

The findings from both SEM observations and XRD analyses support the presence of ettringite and potential thaumasite in the concrete mixtures exposed to 5 °C. The results further indicate a correlation between the mass loss and increase in length, which can be attributed to the formation of thaumasite. This crystalline phase leads to the degradation of the cement matrix, causing material dissociation for some specimens and fracture in others, as ~~confirmed~~ shown by visual observations and the mass-length variation. The

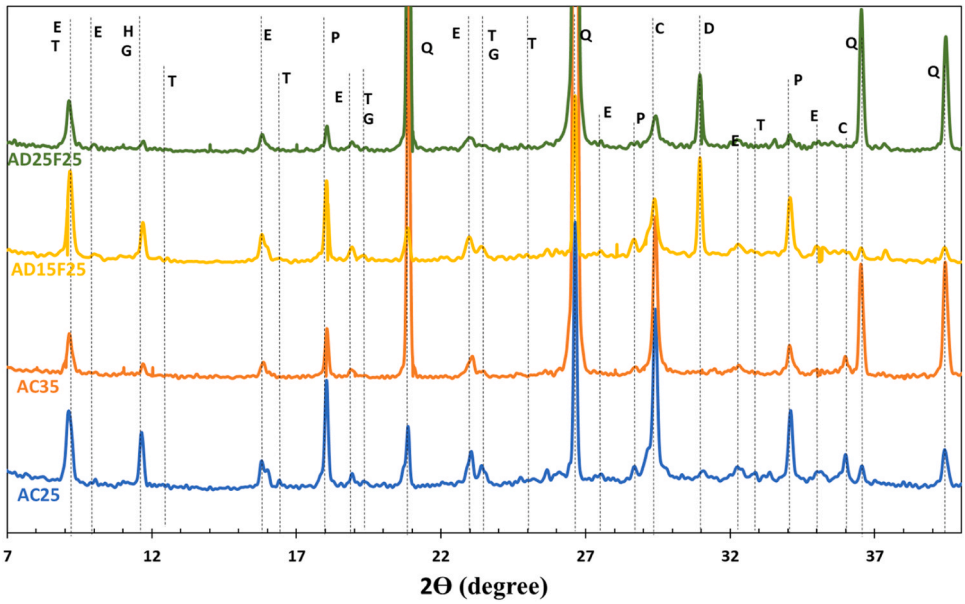

Fig. 12. XRD patterns at the age of 7 months, E: ettringite/ H: hydrotalcite/ T: thaumasite / G: gypsum/ Q: quartz/ C: calcite/ P: portlandite/ D: Dolomite.

distinct behavior observed in the length-mass loss graph is of significant importance as it highlights the different mechanisms operating at 5 °C compared to 23 °C under sulfate exposure.

4. Conclusion

This research presents an innovative approach to evaluate the durability of cementitious materials in the context of Thaumasite Sulfate Attack (TSA), with a particular focus on its applicability to concreting process for deep foundation techniques. Accelerated testing conducted on mortars mixtures designed with 41 different cement-based binders provides valuable insights into the suitability of testing conditions and monitoring parameters for assessing TSA.

- Possible thaumasite attack was observed in various mixtures at 5 °C. This observation was supported by visual degradation, significant mass loss in some specimens, and deterioration in others. SEM/EDX analyses suggested the presence of thaumasite, elucidating its role in the deterioration mechanism at 5 °C, which differs from the typical external sulfate attack observed at 23 °C. Other macroscopic observations on all the specimens at 5 °C were consistent with the phenomenology of TSA.
- For non-sulfate resistant cement (ordinary Portland cement) and limestone filler mixtures, significant TSA was observed starting at 15 % filler content, with more pronounced effects at 25 %, particularly at 5 °C. Additionally, external sulfate attack appeared when filler content exceeded 15 %.

- The type of filler had a significant impact on TSA, whereas its effect on sulfate attack at 23 °C was relatively minor. Mixtures containing dolomite filler showed more pronounced deterioration at 5 °C compared to those with limestone filler. For sulfate resistant cement (cement B) and limestone filler mixtures, significant degradation was observed at 5 °C when the limestone filler content was 25 % or higher. Cement mixtures containing metakaolin ($\geq$ 25 %) or blast furnace slag ($\geq$ 50 %) demonstrated better performance at 5 °C up to 35 % filler content. The presence of fly ash did not prevent TSA at 5 °C; however, mixtures containing fly ash effectively resisted to sulfate attack at 23 °C.
- Relying solely on the 0.1 % length threshold to evaluate TSA resistance at 5 °C was found inadequate. Establishing a mass loss threshold appear necessary to consider thaumasite formation and to assess more reliably resistance to TSA.

The experimental results offer significant information about the behavior of given mortar mixtures. The combination of length and mass variations make it possible to distinguish the particular mechanism corresponding to thaumasite sulfate attack. The use of mortar samples allows keeping the influence of aggregates and defining macroscopic indicators, however a quantitative microscopic analysis is not possible due to the influence of fine aggregates on some characterization techniques. A study on cement paste samples is needed to confirm the findings of microscopic investigations.

CRediT authorship contribution statement

Stéphane Guerineau: Writing – review & editing, Resources, Methodology, Investigation, Conceptualization. **Farah Kaddah:** Writing – original draft, Visualization, Formal analysis, Data curation. **Sonia Boudache:** Writing – original draft, Visualization. **Faten Souayfan:** Writing – original draft, Visualization, Formal analysis, Data curation. **Christophe Justino:** Supervision, Project administration, Funding acquisition. **Emmanuel Roziere:** Writing – original draft, Supervision, Methodology, Conceptualization.

Declaration of Competing Interest

The authors declare that they have no known competing financial interests or personal relationships that could have appeared to influence the work reported in this paper.

Acknowledgements

The authors would like to thank Soletanche and Ecole Centrale de Nantes for their technical and financial support.

Data availability

Data will be made available on request.

References

[1] N. Crammond, The occurrence of thaumasite in modern construction – a review, Cem. Concr. Compos. 24 (3-4) (2002) 393–402, https://doi.org/10.1016/S0958-9465(01)00092-0.
[2] M.M. Rahman, et, M.T. Bassuoni, Thaumasite sulfate attack on concrete: mechanisms, influential factors and mitigation, Constr. Build. Mater. 73 (2014) 652–662, https://doi.org/10.1016/j.conbuildmat.2014.09.034.
[3] N. Rabahi-Touloum, A. Brara, The occurrence of thaumasite in newly built concrete constructions under the semi-arid climate of northeastern Algeria, Mater. Struct. Avr 54 (2) (2021) 69.
[4] R.G. Sibbick, N.J. Crammond, et, D. Metcalf, The microscopical characterisation of thaumasite, Cem. Concr. Compos. 25 (8) (2003) 831–837, https://doi.org/10.1016/S0958-9465(03)00109-4.
[5] P. Brown, et, R.D. Hooton, Ettringite and thaumasite formation in laboratory concretes prepared using sulfate-resisting cements, Cem. Concr. Compos. 24 (3-4) (2002) 361–370, https://doi.org/10.1016/S0958-9465(01)00088-9.
[6] T. Schmidt, B. Lothenbach, M. Romer, J. Neuenschwander, et, K. Scrivener, Physical and microstructural aspects of sulfate attack on ordinary and limestone blended portland cements, Cem. Concr. Res. 39 (12) (2009) 1111–1121, https://doi.org/10.1016/j.cemconres.2009.08.005.
[7] K. Sotiriadis, P. Mácová, A.S. Mazur, A. Viani, P.M. Tolstoy, et, S. Tsivilis, Long-term thaumasite sulfate attack on Portland-limestone cement concrete: a multi-technique analytical approach for assessing phase assemblage, Cem. Concr. Res. 130 (2020) 105995, https://doi.org/10.1016/j.cemconres.2020.105995.
[8] E.N., British Standard, « 197-1. Cement–Part 1: Composition, specifications and conformity criteria for common cements. », London: European Committee For Standardisation, 2011.
[9] K. Sotiriadis, A. Mazur, P. Tolstoy, et, D. Frankeová, Chloride effect on sulfate attack in hydrated Portland-limestone cement assessed by 29Si NMR spectroscopy and thermal analysis, Mater. Today Proc. (2023), https://doi.org/10.1016/j.matpr.2023.06.185.
[10] CSA A3001, « Cementitious materials for use in concrete. Toronto, Ontario: Canadian Standards Association », 2008.
[11] ASTM Standard C595, « Standard specification for blended hydraulic cements. », West Conshohocken, PA: ASTM International, 2012.
[12] EN206, « Concrete – Specification, performance, production and conformity,CEN/TC 104 », 2016, Brussels.
[13] N.J. Crammond, The thaumasite form of sulfate attack in the UK, Cem. Concr. Compos 25 (8) (2003) 809–818, https://doi.org/10.1016/S0958-9465(03)00106-9.
[14] CSA A23.1, « Concrete materials and methods of concrete construction. », Toronto, Ontario: Canadian Standards Association, 2009.
[15] S. Mirvalad, et, M. Nokken, Minimum SCM requirements in mixtures containing limestone cement to control thaumasite sulfate attack, Constr. Build. Mater. 84 (2015) 19–29, https://doi.org/10.1016/j.conbuildmat.2015.02.074.
[16] F. Bellmann, et, J. Stark, Prevention of thaumasite formation in concrete exposed to sulphate attack, Cem. Concr. Res. 37 (8) (2007) 1215–1222, https://doi.org/10.1016/j.cemconres.2007.04.007.
[17] T. Hooton, « Sulfate Resistance of Mortar and Concrete Produced with Portland-Limestone Cement and Supplementary Cementing Materials », 2016.
[18] ASTM Standard C1012., « Standard test method for length change of hydraulicccement mortars exposed to a sulfate solution, vol. 04.01 ». West Conshohocken (PA): ASTM International, 2013.
[19] ASTM Standard C778., « Standard specification for standard sand». ASTM International, 2021.
[20] ASTM C490., « Length change testing of cement, mortar and concrete». ASTM International, 2021.
[21] R. El-Hachem, E. Rozière, F. Grondin, A. Loukili, New procedure to investigate external sulphate attack on cementitious materials, Cem. Concr. Compos. 34 (3) (2012) 357–364.
[22] NF EN 206 + A2/CN Béton - Spécification, performance, production et conformité. Novembre 2022.
[23] C. Yu, W. Sun, et, K. Scrivener, Mechanism of expansion of mortars immersed in sodium sulfate solutions, Cem. Concr. Res. 43 (2013) 105–111, https://doi.org/10.1016/j.cemconres.2012.10.001.
[24] Q. Wang, W. Wilson, et, K. Scrivener, Unidirectional penetration approach for characterizing sulfate attack mechanisms on cement mortars and pastes, Cem. Concr. Res. 169 (2023) 107166, https://doi.org/10.1016/j.cemconres.2023.107166.
[25] A.M. Ramezanianpour, et, R.D. Hooton, Thaumasite sulfate attack in portland and Portland-limestone cement mortars exposed to sulfate solution, Constr. Build. Mater. 40 (2013) 162–173, https://doi.org/10.1016/j.conbuildmat.2012.09.104.
[26] CSA A3004-C8, « Test method for determination of expansion of blended hydraulic cement mortar bars due to external sulphate attack. CSA A3000. Cementitious materials compendium. —Update No. 3 », Canadian Standards Association, Toronto, Ontario, 2011.
[27] NF EN 12390-1, « Testing hardened concrete - Part 1: shape, dimensions and other requirements for specimens and moulds », AFNOR, 2012.
[28] NF EN 12390-3, « Testing hardened concrete - Part 3: compressive strength of test specimens », AFNOR, 2019.
[29] S.J. Barnett, D.E. Macphee, E.E. Lachowski, et, N.J. Crammond, XRD, EDX and IR analysis of solid solutions between thaumasite and ettringite, Cem. Concr. Res. 32 (5) (2002) 719–730, https://doi.org/10.1016/S0008-8846(01)00750-5.
[30] T. Schmidt, B. Lothenbach, M. Romer, K. Scrivener, D. Rentsch, et, R. Figi, A thermodynamic and experimental study of the conditions of thaumasite formation, Cem. Concr. Res. 38 (3) (2008) 337–349, https://doi.org/10.1016/j.cemconres.2007.11.003.

[31] E.F. Irassar, Sulfate attack on cementitious materials containing limestone filler — a review, Cem. Concr. Res. 39 (3) (2009) 241–254, https://doi.org/10.1016/j.cemconres.2008.11.007.
[32] N.J. Crammond, W. Wd, C.D. Pomeroy, Thaumasite in failed cement mortars and renders from exposed brickwork, Cem. Concrc. Res. 15 (1985) 1039–1050.
[33] S.A. Hartshorn, J.H. Sharp, et, R.N. Swamy, Thaumasite formation in Portland-limestone cement pastes, Cem. Concr. Res. 29 (8) (1999) 1331–1340, https://doi.org/10.1016/S0008-8846(99)00100-3.
[34] S. Zhang, Z. Ghouleh, A. Azar, Y. Shao, Improving concrete resistance to low temperature sulfate attack through carbonation curing, Mater. Struct. F. évr 54 (1) (2021) 37.
[35] M. Liu, H. Lu, C. Wang, Y. Liu, An experimental study on microanalytical characterizations and service performances of landfill modified municipal sludge liner materials in contact with leachate, Case Stud. Constr. Mater. 18 (2023) e01794, https://doi.org/10.1016/j.cscm.2022.e01794.
[36] K. Sotiriadis, M. Hlobil, A. Viani, P. Mácová, et, M. Vopálenský, Physical-chemical-mechanical quantitative assessment of the microstructural evolution in Portland-limestone cement pastes exposed to magnesium sulfate attack at low temperature, Cem. Concr. Res. 149 (nov. 2021) 106566, https://doi.org/10.1016/j.cemconres.2021.106566.
[37] N.J. Crammond, The thaumasite form of sulfate attack in the UK, Cem. Concr. Compos 25 (8) (2003) 809–818, https://doi.org/10.1016/S0958-9465(03)00106-9.
[38] F.A. Selim, M.S. Amin, M. Ramadan, et, M.M. Hazem, Effect of elevated temperature and cooling regimes on the compressive strength, microstructure and radiation attenuation of Fly ash–cement composites modified with miscellaneous nanoparticles, Constr. Build. Mater. 258 (oct. 2020) 119648, https://doi.org/10.1016/j.conbuildmat.2020.119648.
[39] S. Boudache, E. Rozière, A. Loukili, et, L. Izoret, Towards common specifications for low- and high-expansion cement-based materials exposed to external sulphate attacks, Constr. Build. Mater. 294 (2021) 123586, https://doi.org/10.1016/j.conbuildmat.2021.123586.
[40] X. Song, Y. Ma, Long-term thaumasite sulfate attack on mortar containing coral sand filler and SCMs exposed to sodium sulfate solution, Case Stud. Constr. Mater. 19 (2023) e02576, https://doi.org/10.1016/j.cscm.2023.e02576.
[41] M. Kobayashi, K. Takahashi, Y. Kawabata, T.A. Bier, Physicochemical properties of portland cement/calcium aluminate cement/calcium sulfate ternary binder exposed to long-term deep-sea conditions, Mater. Struct. Sept. 55 (7) (2022) 182.
[42] M.C.G. Juenger, et, R. Siddique, Recent advances in understanding the role of supplementary cementitious materials in concrete, Cem. Concr. Res. 78 (2015) 71–80, https://doi.org/10.1016/j.cemconres.2015.03.018.
[43] K. RAMYAR, G. INAN, Sodium sulfate attack on plain and blended cements, Build. Environ. 42 (2005) 1368–1372.
[44] R. El-Hachem, E. Rozière, F. Grondin, A. Loukili, Multi-criteria analysis of the mechanism of degradation of portland cement based mortars exposed to external sulphate attack, Cem. Concr. Res. 42 (2012) 1327–1335, https://doi.org/10.1016/j.cemconres.2012.06.005.
[45] G. Artioli, et, J.W. Bullard, Cement hydration: the role of adsorption and crystal growth, Cryst. Res. Technol. 48 (10) (oct. 2013) 903–918, https://doi.org/10.1002/crat.201200713.
[46] F. Deschner, B. Lothenbach, F. Winnefeld, et, J. Neubauer, Effect of temperature on the hydration of portland cement blended with siliceous Fly ash, Cem. Concr. Res. 52 (oct. 2013) 169–181, https://doi.org/10.1016/j.cemconres.2013.07.006.
[47] W. Müllauer, R.E. Beddoe, et, D. Heinz, Sulfate attack expansion mechanisms, Cem. Concr. Res. 52 (oct. 2013) 208–215, https://doi.org/10.1016/j.cemconres.2013.07.005.
[48] S. Boudache, A. Loukili, E. Rozière, et, L. Izoret, Influence of initial material properties on the degradation of mortars with low expansion cements subjected to external sulfate attack, Mater. Struct. 54 (3) (2021) 104, https://doi.org/10.1617/s11527-021-01709-7.
[49] M. Collepardi, A state-of-the-art review on delayed ettringite attack on concrete, Cem. Concr. Compos 25 (4-5) (2003) 401–407, https://doi.org/10.1016/S0958-9465(02)00080-X.
[50] G.W. Scherer, Stress from crystallization of salt, Cem. Concr. Res. 34 (9) (sept. 2004) 1613–1624, https://doi.org/10.1016/j.cemconres.2003.12.034.
[51] B. Tian, M.D. Cohen, et al., Does gypsum formation during sulfate attack on concrete lead to expansion? Cem. Concr. Res. 30 (1) (2000) 117–123, https://doi.org/10.1016/S0008-8846(99)00211-2.
[52] L. Qin, X. Mao, X. Gao, P. Zhang, T. Chen, Q. Li, Y. Cui, Performance degradation of CO2 cured cement-coal gangue pastes with low-temperature sulfate solution immersion, Case Stud. Constr. Mater. 17 (2022) e01199, https://doi.org/10.1016/j.cscm.2022.e01199.
[53] S.J. Barnett, D.E. Macphee, E.E. Lachowski, et, N.J. Crammond, XRD, EDX and IR analysis of solid solutions between thaumasite and ettringite, Cem. Concr. Res. 32 (5) (2002) 719–730, https://doi.org/10.1016/S0008-8846(01)00750-5.
[54] R. Komatsu, N. Mizukoshi, K. Makida, K. Tsukamoto, In-situ observation of ettringite crystals, J. Cryst. Growth 311 (2009) 1005–1008, https://doi.org/10.1016/j.jcrysgro.2008.09.124.
[55] S. Mantellato, M. Palacios, R.J. Flatt, Impact of sample preparation on the specific surface area of synthetic ettringite, Cem. Concr. Res. 86 (2016) 20–28, https://doi.org/10.1016/j.cemconres.2016.04.005.
[56] M.T. Bassuoni, M.L. Nehdi, et al., Durability of self-consolidating concrete to sulfate attack under combined cyclic environments and flexural loading, Cem. Concr. Res. 39 (3) (2009) 206–226, https://doi.org/10.1016/j.cemconres.2008.12.003.
[57] F. Liu, W. Cao, T. Yang, J. Xu, D. Lu, R.D. Hooton, Sulfate attack on portland-dolomite cement exposed to sodium sulfate solution at 5 ℃ and 20 ℃, Case Stud. Constr. Mater. 21 (2024) e03894 https://doi.org/10.1016/j.cscm.2024.e03894.